Dickinson LR, Kranbuehl DE and Schniepp HC (2016) Assessing graphene oxide/polymer interfacial interactions by way of peeling test. *Surface Innovations* **4(3)**: 158–166, http://dx.doi.org/10.1680/jsuin.16.00009

Surface Innovations
Volume 4 Issue SI3
Research Article
Received 19/07/2016 Accepted 05/09/2016
Published online 21/09/2016
Keywords: interface/microscopy/nanocomposites

ice | science

ice Institution of Civil Engineers publishing

Assessing graphene oxide/polymer interfacial interactions by way of peeling test

1 **Laura R. Dickinson** PhD
Research Assistant, Department of Applied Science, The College of William & Mary, Williamsburg, VA, USA

2 **David E. Kranbuehl** PhD
Professor, Department of Chemistry, The College of William & Mary, Williamsburg, VA, USA

3 **Hannes C. Schniepp** Dr. sc. nat.*
Adina Allen Term Distinguished Associate Professor, Department of Applied Science, The College of William & Mary, Williamsburg, VA, USA



The design of graphene/polymer nanocomposites with improved mechanical properties requires characterization of the interfacial interactions between different types of graphene sheets and different polymers. In this study, the interactions in a graphene oxide (GO)/polymer nanocomposite were explored and the effect of thermal reduction of GO on adhesion was tested. A versatile peeling test was demonstrated and applied on a wide range of nanosheet fillers and polymers, which has great potential for expedited development of enhanced nanocomposites. The interactions of GO and reduced graphene oxide (rGO) nanofillers were tested with widely used polymers, including poly(methyl methacrylate), polystyrene, acrylic, polyvinyl alcohol, polyetherimide and polyimide. The results show the effect of thermal reduction of GO on the interactions in polymer nanocomposites and rank the interfacial preferences of GO and rGO for different polymers. In terms of surface energy considerations, some of the results are in agreement with expectations, others are in direct contradiction. This discrepancy suggests that molecular-level effects, which are not reflected in the macroscopic material properties, play a significant role.

1. Introduction/background

Polymer nanocomposites offer an opportunity to design high-performance lightweight materials[1] and can provide additional functionalities.[2,3] Improvement in the ability to tailor the properties of such materials easily and rapidly would have significant impact on many engineering applications, such as transportation and structures.[4] It has been widely appreciated that it is crucial in matrix–filler nanocomposites for the interfacial bonding to be strong enough to transfer stress from the matrix to the filler effectively.[5] In most cases, the macroscopic mechanical characteristics of the nanocomposites were studied, thereby assessing the interfacial bonds indirectly. Techniques used to study the structural properties have included tensile tests,[6] dynamic mechanical thermal analysis,[7] dynamic mechanical analysis,[8] shaft-loaded blister method,[9] strain-induced elastic buckling instability for mechanical measurements,[10] the copper grid technique,[11] the notched Izod test[12] and the compact tension method.[7] Additionally, techniques such as nanoindentation[13] and 'nanoscratch'[13] provide a more microscopic measurement, but are still probing properties such as Young's modulus in sample volumes much larger than the size of the filler nanoparticles and thus provide properties averaged over the nanofillers and the matrix, similar to macroscopic measurements.

Macroscopic characterization of the mechanical properties of the resulting material, such as tensile testing, is important because ultimately, it is these properties that researchers strive to optimize. However, since such tests do not directly measure the matrix–filler interactions, they do not provide any insights into the nanomechanics of such composite materials. Properties are averaged over the entire test specimen, and the macroscopic data alone do not provide information to explain the observed performance. For instance, a low strength could be due to matrix failure, due to rupturing of the nanofillers, due to weak matrix–filler adhesion or due to imperfect dispersion of the nanofiller particles. This lack of direct information about

***Corresponding author e-mail address:** schniepp@wm.edu

performance at the scale of the filler particles thus hampers the optimization of systematic materials, which is instead done by trial and error. In order to probe matrix–filler interactions directly in such systems, a number of experimental approaches have been proposed. Experimentally, this is challenging, since the filler particles are very small in the case of nanocomposites. Additionally, the filler particles are difficult to access since they are embedded within the polymer matrix.

Some groups have addressed these problems by performing atomic force microscopy (AFM) pullout experiments;[14] other researchers have used transmission electron microscopy (TEM)[6,15] and scanning electron microscopy[15] to observe the effect of a nanofiller on fracture patterns. In one case, the researchers used TEM after a fracture test to show that nanotubes had pulled out of the polymer but retained a polymer coating, showing that the nanotube/polymer bond was greater than the bond between polymer molecules.[16] Another group used an AFM probe to measure the force required to scratch a thin layer of polymer off a nanofiller platelet.[17] Still, other researchers have utilized Raman spectroscopy to prove that stress in the polymer matrix is being transferred directly to the nanofiller.[18]

This work focused on studying the interactions of individual flakes of graphene oxide (GO) or reduced graphene oxide (rGO) with several widely used polymers. Nanocomposites made out of these materials have great potential for industrial and commercial applications.[19] However, many polymers are available, as well as graphene sheets with different surface functionalizations,[20,21] and it is challenging to predict which polymer/nanofiller combination will exhibit strong interfacial interactions and thus make a successful nanocomposite. Techniques for direct assessment of these interactions for plate-like nanofillers, on the other hand, are very limited. For example AFM pullout experiments are not suitable for the platelet morphology of GO. The AFM polymer-scratching technique provides information on forces applied laterally between the polymer and platelet, but not for forces applied normal to the platelet. Raman spectroscopy provides the matrix–filler strain, but does not directly measure the force between the GO and the polymer.

In order to address this problem, the authors have recently developed a method that allows a quick and efficient study of the interfacial interactions between nanosheet materials and polymers.[22,23] By utilizing this approach, the authors addressed two main objectives in this work: (*a*) create a ranking of the affinity of GO and rGO for multiple polymers and (*b*) determine the effect of thermal reduction of GO to rGO on interfacial interactions with several polymers. Understanding the effect of GO reduction is vital, since the processing of nanocomposites requires a range of temperatures, including some that are high enough to thermally reduce GO on site.[24] As GO reduces to rGO, the carboxyl and hydroxyl functional groups on its surface are removed at temperatures lower than those for the epoxides.[25] Therefore, the degree of reduction has a significant effect on how the rGO will interact with the polymer. Additionally, since rGO can exhibit a topography more wrinkled than that of GO,[26] the differences between the geometry of these two materials might lead to different interactions with the polymers.[1]

By performing measurements with multiple nanofiller/polymer combinations, the authors have developed a ranking of the affinity of GO and rGO for particular polymer systems. To make these results pertinent to commercial applications, the authors utilized some of the most common industrial polymers available: polystyrene (PS), polyetherimide (PEI), polyimide (PI), poly (methyl methacrylate) (PMMA), polyvinyl alcohol (PVA) and an acrylic utilized in paint. By choosing such well-known polymers and studying the effects of thermal reduction of GO nanofillers on interfacial adhesion, the authors introduce directly applicable and relevant information to facilitate other researchers in advancing the progress of nanocomposite development.

2. Experimental

2.1 Sample preparation

The three essential components in this study's peeling tests involved (*a*) a substrate, (*b*) a nanosheet material and (*c*) a polymer. First, the nanosheet materials were casted onto the substrates by way of a spin processor (Laurell WS-400Bz-6NPP-Lite spin processor) from liquid dispersions. Then, the polymer was added on top in the form of a polymer solution and left to dry. Once all of the solvent had evaporated and the polymer had dried into a solid film, it was mechanically peeled off the substrate. Finally, the surfaces were analyzed by way of AFM to determine to which side the nanosheet material adhered.

As substrates, mica, highly oriented pyrolitic graphite (HOPG) and mica functionalized with a non-polar compound were utilized. Mica (Ted Pella; Pelco, grade V5) and HOPG (NT-MDT; ZYH quality) were freshly cleaved directly before each experiment. To functionalize mica, a piece of freshly cleaved mica was placed in a desiccator with a 3 µl droplet of (tridecafluoro-1,2,2-tetrahydrooctyl) trichlorosilane (Gelest, Inc.) for 2 h to evaporate. After functionalization, the silanized mica was stored in closed containers.

The GO was produced using both the Hummers[27] and improved Hummers methods,[28] using grade 3243 graphite from Asbury Carbons and graphite flakes from Sigma-Aldrich. GO was thermally reduced to rGO by employing three different routes, depending on the sample (see Table 1). In some cases, GO was thermally reduced before application to the substrate by heating it for 10 min at 400°C in air in a Thermolyne 47900 furnace. In other cases, it was reduced on the substrate by using a hot plate for 60 min at 240°C before adding the polymer under an argon flow. For the rGO/PEI and rGO/PI samples, finally, the GO was reduced on site as the polymers thermally cured (see details in the following paragraph). The nanosheet materials were dispersed using a range of solvents, including *N*-methyl-2-pyrrolidone (Acros Organics), dimethylformamide (DMF; Acros Organics), dimethylacetamide

Nanosheet material	Method of preparation
GO	Hummers[27] and improved Hummers[28]
rGO (on site for PI)	Details in text
rGO (reduced before application to substrate for PVA and PMMA tests)	Heating of GO for 10 min at 400°C
rGO (on site for PEI)	Heated sample for 30 min at 250°C
rGO (reduced on substrate before acrylic application)	Heating of GO-coated substrate for 60 min at 240°C

Table 1. Details of processing methods for nanosheet materials used in the peeling tests

(DMAc; Sigma-Aldrich) and double-deionized water (Millipore Synergy UV). Spin-casting these dispersions distributed single-layer nanosheets on the substrates with negligible overlap.

The employed polymers were PI, PMMA (Sigma-Aldrich; M_W 120 000), PVA (Sigma-Aldrich; Mowiol 4-88), PEI (DuPont; Ultem 1000), PS (Sigma-Aldrich; M_W 230 000) and acrylic (Rhoplex HG-706). Except for PI and acrylic, the polymers were dissolved in solvents (see Table 2; solvent sources same as for nanosheet dispersion; toluene was from Fisher Scientific (Optima)) and then pipetted on top of the sheets to cover the substrates fully and left to dry. In case of the acrylic, the Rhoplex HG-706 acrylic formulation was directly pipetted onto the substrate and left to dry. For PI, a more elaborate protocol was used, as discussed in the following. Poly(amic acid) was first made using DMAc, benzophenone-3,3′,4,4′-tetracarboxylic dianhydride and 4,4′-oxydianiline, as described in the literature.[29] The poly(amic acid) was then applied to the substrate, and the sample was put in a Thermolyne 47900 furnace; heated to 100°C at a rate of 3°C/min, with the temperature retained for 1 h; and then further heated to 300°C at a rate of 1·67°C/min, with the temperature retained for 1 h. Finally, the sample was cooled down to ambient temperature at a slow rate of −15°C/min.

To perform the peeling, a scalpel was inserted between the substrate and one edge of the film for separation. An exception was PI, which was rolled into a tube peeled in this manner. To stabilize this comparatively thinner film, a metal disk was first adhered to the upper side of the PI by using an adhesive tab, allowing the tab to be peeled off in the same manner as the other polymers.

2.2 Atomic force microscopy

AFM (NT-MDT; Ntegra Prima) was used in ambient conditions to scan the substrates and/or polymers to identify the location of the flakes after peeling. The polymer films were inverted to study the side of the film previously in contact with the sheets. Contact and dynamic modes were used, including force modulation microscopy (FMM). For contact mode, silicon nitride probes (SiNi, BudgetSensors) featuring tip radii of curvature <15 nm and two cantilever types with nominal spring constants of 0·27 and 0·06 N/m and resonance frequencies of 30 and 10 kHz were used. For dynamic-mode scans, Acta probes (AppNano) with tip radii <10 nm, nominal spring constants of 40 N/m and resonance frequency of 300 kHz were used. For FMM, Tetra 18 probes (K-Tek Nanotechnology) with tip radii <50 nm, nominal spring constant of 5 N/m and resonance frequency of 100 kHz were used.

3. Results

3.1 Polyetherimide

Tests with (unreduced) GO on mica and HOPG were first performed. AFM images of the PEI surface that was in contact with HOPG prior to peeling showed flake-shaped depressions in the height image (dark areas in Figure 1(a)). As previously discussed,[22,23] this indicates sheets sticking more strongly to the substrate than to the polymer upon peeling. However, lateral force images of the PEI surface also show a few flakes adhering to the PEI (light-colored areas circled in Figure 1(b)), which were apparently peeled off from HOPG. This indicates that GO interacts more strongly with HOPG than with PEI, albeit at a relatively small difference of interactions, since a minority of sheets stuck more strongly to PEI than to HOPG.

Polymer	Liquid polymer solution method	Drying/curing temperature
PI	Discussed in the text	300°C
PMMA	20 wt% PMMA/80 wt% DMF	90°C
PVA	20 wt% PVA/80 wt% water	50°C
PEI	20 wt% PEI/80 wt% DMAc	90°C
PS	20 wt% PS/80 wt% toluene	50°C
Acrylic	Applied directly to substrate	Ambient temperature

Table 2. Details of how the polymer solutions were made (solvents, concentrations) and how they were dried/cured on the nanosheet-coated substrates

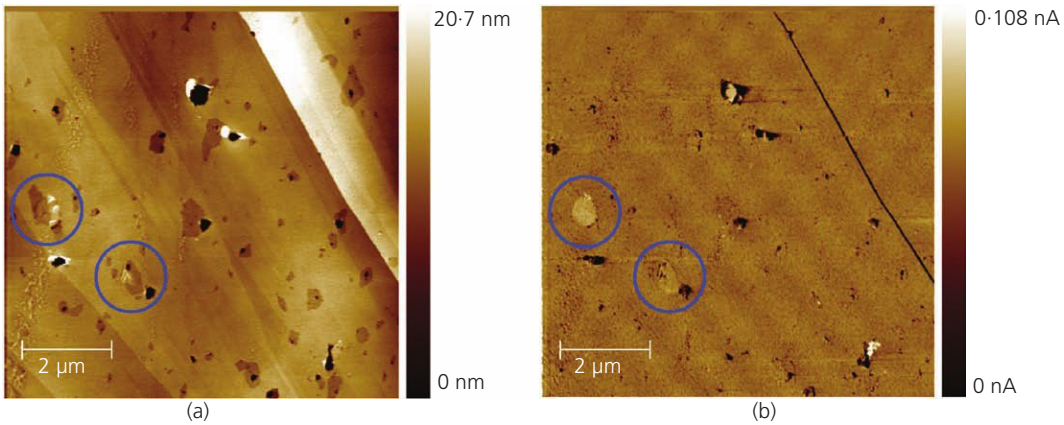

Figure 1. AFM images of PEI after peeling off a GO/HOPG substrate. In the height image of the PEI surface (a), there are many depressions visible due to the sheets remaining attached to the HOPG. In the lateral force image (b), there are a few sheets that were peeled off with the PEI (indicated by blue circles). The blue circles in (a) and (b) indicate the same locations

For the GO/mica/PEI system, AFM scans of the PEI surface also revealed flake-shaped depressions in the height image (Supplementary Material Figure S1). However, for the mica, none of the flakes remained attached to the PEI. Since all the GO flakes remained attached to the mica, it can be concluded that GO interacts significantly more strongly with mica than with PEI. Since for the GO/HOPG/PEI system most but not all of the GO flakes remained attached to HOPG, the following order of interaction strengths of several materials with GO can be established: mica > HOPG > PEI. To study the effects of thermal reduction, peeling tests with rGO reduced on site in PEI on mica were also performed. Interestingly, the rGO reduced on site for PEI remained entirely embedded in the polymer and retained the same appearance of the flakes. By remaining attached to the PEI as it was peeled off the mica (Supplementary Material Figure S1), rGO exhibited a trend reversal from results that had been observed in the GO/mica/PEI system.

3.2 Poly(methyl methacrylate)

To study the interactions of rGO and PMMA, an rGO/mica/PMMA peeling test was performed. By scanning the PMMA surface by using the FMM mode, rGO flakes embedded in PMMA were detected (Supplementary Material Figure S2). FMM detects local sample stiffness and thus is a powerful imaging mode for detecting material differences even when a sample has no or little topography, such as in the case of graphene sheets that are embedded flush with the polymer surface. Since graphene is much stiffer than typical polymers, FMM often shows significant contrast for such samples.

These experiments show that the rGO sheets peeled off with the polymer, which demonstrates that the rGO/PMMA interaction was stronger than the rGO/mica interaction. This development directly shows the effect of thermal reduction on rGO/PMMA interactions. In the authors' previous study, it was found that[23] the GO/mica interaction was stronger than the GO/PMMA interaction; now, the rGO/PMMA interaction is stronger than the rGO/mica interaction. Therefore, thermal reduction caused the nanosheets to switch their preference from mica to PMMA.

3.3 Polyvinyl alcohol

To study the effect of thermal reduction of GO to rGO on interactions with PVA, rGO was applied to a mica substrate and the peeling test was performed. Although a few rGO sheets adhered to the PVA (Supplementary Material Figure S2), most remained on the mica. This directly showed the effect of thermal reduction in the rGO/PVA system: reducing the GO switches the adhesion preference of the nanofiller from PVA[23] to mica.

3.4 Polystyrene

Peeling tests with GO on mica and HOPG were performed by using PS. For the GO/HOPG/PS system, the GO remained attached to the HOPG, leaving behind flake-shaped depressions in the PS (Supplementary Material Figure S2). By examining the PS peeled from mica (Figure 2), many similar depressions left by the flakes were seen. However, a few flakes adhered to the PS and peeled off the mica (indicated by blue circles), showing that the interactions in the GO/mica/PS system are similar, but that the GO/mica interaction is stronger than the GO/PS interaction. Based on these results, the trend for the relative interaction strengths is GO/HOPG > GO/mica > GO/PS.

3.5 Acrylic

Acrylic was studied as it is widely used in paints; enhancing its mechanical and barrier properties thus holds great practical value for commercial products. In this study, peeling tests with GO on mica and silanized mica were performed; in both cases, the GO stuck to the substrates. For this polymer, AFM scans of the very same location on the substrate were carried out before employing the polymer and after peeling it off. This allowed tracking every single graphene sheet without scanning the polymer surface after peeling. For mica, each individual flake was visible before and after peeling (see Supplementary Material Figure S3). Results for

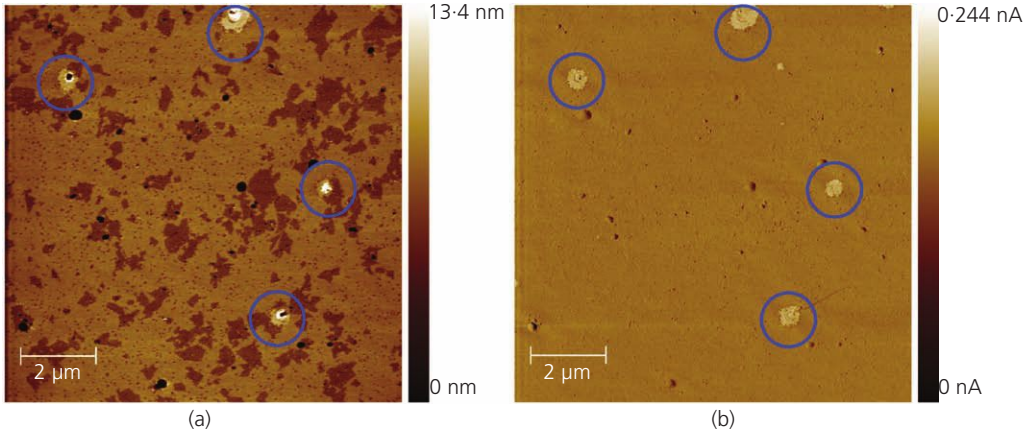

Figure 2. AFM images of PS after peeling off a GO/mica substrate. Depressions are visible in the polymer surface in the height image (a). The lateral force image (b) shows a few flakes sticking to PS (indicated in both images by blue circles)

the silanized mica are shown in Figures 3(a) and 3(b), featuring the same location before and after peeling, with only one flake missing after peeling (indicated by the blue circle). Thermal reduction of GO to rGO on a mica substrate prior to applying acrylic did not change the adhesion preference: rGO still stuck to mica in an rGO/mica/acrylic test.

3.6 Polyimide

For PI, the polymer was thermally cured on the GO-covered substrate and then peeled off, with temperatures high enough to thermally reduce GO to rGO on site (see Section 2). Peeling tests were performed on mica and silanized mica. For rGO/mica/PI, the flakes peeled off mica, as seen in the FMM image of the peeled PI surface in Figure 4(a), where the flakes (darker areas) are embedded in PI (lighter areas).

For the rGO/silanized mica/PI, in contrast, the flakes stuck to silanized mica. AFM scans of the same location before and after peeling (Figures 4(b) and 4(c)) show the same flakes attached to the silanized mica substrate. To highlight this fact, two blue circles indicate two very distinctive flake shapes in the two images. Interestingly, although the flakes retain the same outline, they appear to have broken into much smaller pieces and have consequently developed a blurry appearance. The exact reason for this is unclear, since the peeling tests for both the mica and the silanized mica were subjected to the same temperatures. Perhaps the flakes embedded in the polymer were also broken into smaller pieces by the thermal treatment, but retained their shape due to the confines of the surrounding PI. Consequently, the interfacial adhesion of rGO with different substrates declines in the following order: silanized mica > PI > mica.

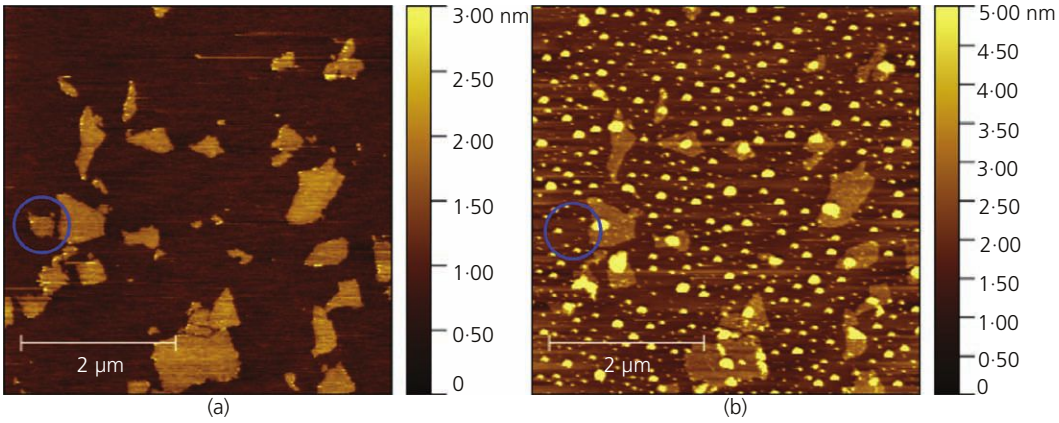

Figure 3. AFM height images of GO sheets on silanized mica (a) before and (b) after peeling off acrylic. Panel (b) shows residue from the acrylic on the surface (bright spots)

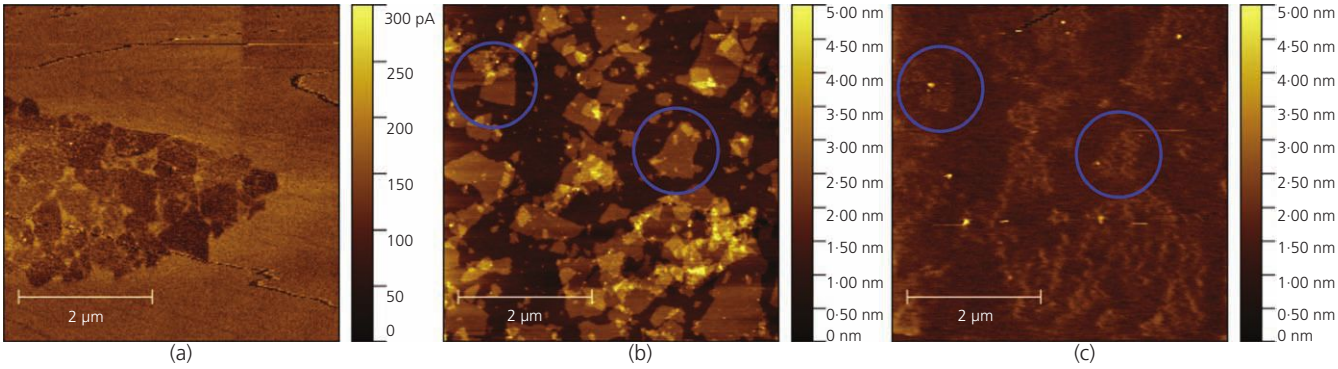

Figure 4. (a) FMM image of PI showing embedded rGO sheets after peeling off a mica substrate. (b) AFM height image of GO on silanized mica. (c) AFM height image of the same location as in (b) after peeling off the PI. Features circled in blue are the same in both (b) and (c)

4. Discussion

To facilitate comparison of these experiments, all peeling resultsare summarized in Table 3. Each row represents one substrate/nanosheet/polymer combination, ordered by polymers as introduced in Section 3. In cases where all sheets adhered to one surface (substrate or polymer), the material is colored yellow. In cases of partial adhesion to substrate and polymer, shades of green were used, with darker greens indicating a greater fraction. Surface energies for each polymer are given in the fourth row.

For PEI, the GO interaction strengths with different materials declined in the following order: mica > HOPG > PEI. Although some authors have suggested that there are other factors important in adhesion,[37] the authors of the present study are considering surface energies to classify and discuss their results. On this basis, it was not surprising that the authors found better adhesion of GO to mica (70–140 mJ/m^2 of surface energy[38]) than to PEI (45–50 mJ/m^2). In contrast, the authors did not expect GO to adhere more strongly to HOPG (18–40 mJ/m^2 of surface energy[39–41]) than to PEI. Once reduced to rGO, the sheets had the strongest interactions in this order: PEI > mica. The authors found this also surprising, due to the significantly lower surface energy of PEI in comparison to that of mica. Consequently, surface energy considerations alone may indeed not be sufficient to assess interfacial interactions of graphene. Molecular level effects not included in such macroscopic descriptions potentially play an important role.

For the PMMA tests, a clear switch was observed in the affinity of the sheets as a function of thermal reduction of GO. GO adhesion declined in the order mica > PMMA > HOPG,[23] which is in line with what the authors would expect according to surface energies, since the PMMA value (36–45 mJ/m^2) is between those for mica and HOPG. For rGO, on the other hand, the order was PMMA > mica. Based on surface energy considerations, this is surprising, since PMMA features a much lower surface energy than mica. This could be due to the molecular structure of PMMA, which has epoxy and ester functional groups, potentially contributing to hydrogen bonding as bond acceptors when interacting with GO.[1,42,43] According to the tests, composites with rGO nanofillers are expected to perform better than GO-filled materials.

In PVA, reduction caused the nanoparticle to switch its preference, but in opposite direction compared to PMMA: adhesions were GO/PVA > GO/mica[23] and rGO/PVA < rGO/mica. Consideration of surface energies is not very useful in this case, as literature values for both mica and PVA (62–95 mJ/m^2) show a significant overlap. At any rate, according to this study's results, PVA nanocomposites are expected to show best performance with unreduced GO.

For the PS system, it was found that the majority, and not all GO sheets, adhered to mica. This is quite surprising since mica has a much higher surface energy (70–140 mJ/m^2) than PS (25–41 mJ/m^2). For HOPG, in contrast, which has a similar or perhaps even lower surface energy (18–40 mJ/m^2), all sheets adhered more strongly on HOPG. Based on this experiment with PS, the adhesion strengths of GO decrease in the order HOPG > mica > PS, which is particularly surprising, since HOPG is the material with the lowest surface energy. It is also not in line with the PMMA experiments, where GO adhered more strongly to mica than to HOPG, as expected.

For the acrylic system, the peeling tests show that both GO and rGO exhibit very poor adhesion, regardless of whether the substrate was mica or silanized mica. To be utilized effectively in a nanocomposite system, a different type of nanofiller with greater interfacial adhesion to the acrylic would have to be used instead. This could be achieved by functionalizing GO flakes with different surface groups in order to maximize adhesion with the acrylic. Since a commercial acrylic formulation

Substrate	Nanosheet	Polymer	Polymer surface energy: mJ/m^2
Mica	GO	PEI	45–50[30,31]
HOPG	GO	PEI	
Mica	rGO[a]	PEI	
Mica	GO	PMMA	36–45[32,33]
HOPG	GO	PMMA	
Mica	rGO[b]	PMMA	
Mica	GO	PVA	62–95[34]
Mica	rGO[b]	PVA	
Mica	GO	PS	25–41[32,35]
HOPG	GO	PS	
Mica	GO	Acrylic	Not available
Silanized mica	GO	Acrylic	
Mica	rGO[c]	Acrylic	
Mica	rGO[a]	PI	37[36]
Silanized mica	rGO[a]	PI	

[a] GO reduced on site during polymer drying/curing.
[b] GO thermally reduced before being applied to the substrate.
[c] GO thermally reduced on the substrate by way of a hot plate, prior to application of the polymer.
In cases where all nanosheets adhered to one material (substrate or polymer), this material is colored yellow. In cases where a fraction of the flakes adhered to each material, the darker/lighter green colors indicate the surfaces carrying the majority/minority of flakes.

Table 3. Summary of peeling test results for all polymer/nanosheet/substrate combinations

was used, no surface energy values were available in the literature.

The PI peeling tests were all performed with rGO since the elevated temperature of the thermal imidization is expected to cause on-site reduction of GO. For this materials system, interfacial adhesions decreased in the following order: silanized mica > PI > mica. Given that PI (37 mJ/m^2) features a much lower surface energy compared to mica, it is surprising that rGO adheres more strongly to PI than to mica.

Finally, a comparison of the adhesion of GO and rGO across different polymers is interesting. Namely, it can be determined that for GO the ranking of decreasing adhesion with an assortment of polymers is PVA > PMMA > PEI ≈ PS. Remarkably, this ranking is perfectly in line with expectations based on surface energies. For rGO, on the other hand, the adhesion ranking is PI ≈ PMMA ≈ PEI > PVA > acrylic. The fact that PI, PMMA and PEI all show similar adhesion values is in line with the fact that the surface energies of these polymers are all similar. However, it is surprising that PVA exhibits weaker adhesion, as it exhibits a higher surface energy than PI, PMMA and PEI.

5. Conclusion

By using the peeling method, the interfacial interactions of two nanofiller materials, GO and rGO, with a range of commonly used polymers were assessed. This allowed ranking the polymers according to their interfacial adhesion with each nanofiller. For PMMA, PVA and PEI, a clear change in the polymer affinity was seen as graphene surface chemistry was changed by way of thermal reduction of functional groups. The results are discussed in terms of surface energies, and it was found that only in some cases the adhesion behavior was in agreement with expectations. In other cases, the findings were in direct contradiction to surface energy considerations. This could mean that molecular level effects, which are not reflected in the macroscopic properties of the materials, play a significant role. These examples demonstrate how crucial it is to have experimental methods such as the peeling test, which enables direct measurement of interfacial interactions in nanocomposites.

Acknowledgements

HCS acknowledges support from the US National Science Foundation under grant numbers DMR-1352542 and 1534428. DEK acknowledges support from the American Chemical

Society's Petroleum Research Fund, grant 542353-ND-7. The authors acknowledge Natalie Hudson-Smith and Hae Seong Kim for the preparation of polyimide and acrylic samples respectively.

REFERENCES

1. Ramanathan T, Abdala AA, Stankovich S *et al.* (2008) Functionalized graphene sheets for polymer nanocomposites. *Nature Nanotech* **3(6)**: 327–331.
2. Fang ZH, Punckt C, Leung EY, Schniepp HC and Aksay IA (2010) Tuning of structural color using a dielectric actuator and multifunctional compliant electrodes. *Applied Optics* **49(35)**: 6689–6696.
3. Hocker S, Hudson-Smith N, Schniepp HC and Kranbuehl DE (2016) Enhancing polyimide's water barrier properties through addition of functionalized graphene oxide. *Polymer* **93**: 23–29.
4. Schadler L (2007) Nanocomposites: model interfaces. *Nature Materials* **6**: 257–258.
5. Young RJ, Kinloch IA, Gong L and Novoselov KS (2012) The mechanics of graphene nanocomposites: A review. *Composites Science and Technology* **72(12)**: 1459–1476.
6. Qian D, Dickey EC, Andrews R and Rantell T (2000) Load transfer and deformation mechanisms in carbon nanotube–polystyrene composites. *Applied Physics Letters* **76(20)**: 2868–2870.
7. Becker O, Varley R and Simon G (2002) Morphology, thermal relaxations and mechanical properties of layered silicate nanocomposites based upon high-functionality epoxy resins. *Polymer* **43(16)**: 4365–4373.
8. Putz KW, Mitchell CA, Krishnamoorti R and Green PF (2004) Elastic modulus of single-walled carbon nanotube/poly (methyl methacrylate) nanocomposites. *Journal of Polymer Science: Part B: Polymer Physics* **42(12)**: 2286–2293.
9. Xu X, Thwe MM, Shearwood C and Liao K (2002) Mechanical properties and interfacial characteristics of carbon-nanotube-reinforced epoxy thin films. *Applied Physics Letters* **81(15)**: 2833–2835.
10. Stafford CM, Harrison C, Beers KL *et al.* (2004) A buckling-based metrology for measuring the elastic moduli of polymeric thin films. *Nature Materials* **3(8)**: 545–550.
11. Crosby AJ and Lee JY (2007) Polymer nanocomposites: the 'nano' effect on mechanical properties. *Polymer Reviews* **47(2)**: 217–229.
12. Akkapeddi MK (2000) Glass fiber reinforced polyamide-6 nanocomposites. *Polymer Composites* **21(4)**: 576–585.
13. Li X, Gao H, Scrivens WA *et al.* (2004) Nanomechanical characterization of single-walled carbon nanotube reinforced epoxy composites. *Nanotechnology* **15(11)**: 1416–1423.
14. Barber AH, Cohen SR and Wagner HD (2003) Measurement of carbon nanotube–polymer interfacial strength. *Applied Physics Letters* **82(23)**: 4140–4142.
15. Wang K, Chen L, Wu J *et al.* (2005) Epoxy nanocomposites with highly exfoliated clay: mechanical properties and fracture mechanisms. *Macromolecules* **38(3)**: 788–800.
16. Cadek M, Coleman JN, Barron V, Hedicke K and Blau WJ (2002) Morphological and mechanical properties of carbon-nanotube-reinforced semicrystalline and amorphous polymer composites. *Applied Physics Letters* **81(27)**: 5123–5125.
17. Aoyama S, Park YT, Macosko CW, Ougizawa T and Haugstad G (2014) AFM probing of polymer/nanofiller interfacial adhesion and its correlation with bulk mechanical properties in a poly(ethylene terephthalate) nanocomposite. *Langmuir* **30(43)**: 12950–12959.
18. Cooper CA, Young RJ and Halsall M (2001) Investigation into the deformation of carbon nanotubes and their composites through the use of Raman spectroscopy. *Composites Part A: Applied Science and Manufacturing* **32(3–4)**: 401–411.
19. Kim H, Abdala AA and Macosko CW (2010) Graphene/polymer nanocomposites. *Macromolecules* **43(16)**: 6515–6530.
20. Glover AJ, Adamson DH and Schniepp HC (2012) Charge-driven selective adsorption of sodium dodecyl sulfate on graphene oxide visualized by atomic force microscopy. *The Journal of Physical Chemistry C* **116(35)**: 20080–20085.
21. Schniepp HC, Li JL, McAllister MJ *et al.* (2006) Functionalized Single graphene sheets derived from splitting graphite oxide. *Journal of Physical Chemistry B* **110(17)**: 8535–8539.
22. Cai M, Glover A, Wallin T *et al.* (2010) Direct measurement of the interfacial attractions between functionalized graphene and polymers in nanocomposites. In *V International Conference on Times of Polymers (Top) and Composites* (D'Amore A, Acierno D and Grassia L (eds)). AIP Conference Proceedings, American Institute of Physics. College Park, MD, USA, vol. 1255, pp. 95–97.
23. Kranbuehl DE, Cai M, Glover AJ and Schniepp HC (2011) Measurement of the interfacial attraction between graphene oxide sheets and the polymer in a nanocomposite. *Journal of Applied Polymer Science* **122(6)**: 3740–3744.
24. Glover AJ, Cai M, Overdeep KR, Kranbuehl DE and Schniepp HC (2011) In situ reduction of graphene oxide in polymers. *Macromolecules* **44(24)**: 9821–9829.
25. Compton OC, Jain B, Dikin DA *et al.* (2011) Chemically Active reduced graphene oxide with tunable C/O ratios. *ACS Nano* **5(6)**: 4380–4391.
26. Schniepp HC, Kudin KN, Li JL *et al.* (2008) Bending properties of single functionalized graphene sheets probed by atomic force microscopy. *ACS Nano* **2(12)**: 2577–2584.
27. Cai M, Thorpe D, Adamson DH and Schniepp HC (2012) Methods of graphite exfoliation. *Journal of Materials Chemistry* **22(48)**: 24992–25002.
28. Marcano DC, Kosynkin DV, Berlin JM *et al.* (2010) Improved synthesis of graphene oxide. *ACS Nano* **4**: 4806–4814.
29. Southward RE, Boggs CM, Thompson DW and St Clair AK (1998) Synthesis of surface-metallized polyimide films via in situ reduction of (perfluoroalkanoato)silver(I) complexes in a poly(amic acid) precursor. *Chemistry of Materials* **10(5)**: 1408–1421.
30. Kaba M, Raklaoui N, Guimon MF and Mas A (2005) Improvement of the water selectivity of ULTEM poly(ether imide) pervaporation films by an allylamine-plasma-polymerized layer. *Journal of Applied Polymer Science* **97(5)**: 2088–2096.

31. Qariouh H, Schué R, Schué F and Bailly C (1999) Sorption, diffusion and pervaporation of water/ethanol mixtures in polyetherimide membranes. *Polymer International* **48(3)**: 171–180.
32. Mark JE (1996) *Physical Properties of Polymers Handbook*. AIP Press, New York, NY, USA.
33. Ozcan C and Hasirci N (2008) Evaluation of surface free energy for PMMA films. *Journal of Applied Polymer Science* **108(1)**: 438–446.
34. Kim JH, Shin DS, Han MH *et al.* (2007) Surface free energy analysis of poly(vinyl alcohol) films having various molecular parameters. *Journal of Applied Polymer Science* **105(2)**: 424–428.
35. Mark JE (1999) *Polymer Data Handbook*. Oxford University Press, New York, NY, USA.
36. Inagaki N, Tasaka S and Hibi K (1994) Improved adhesion between plasma-treated polyimide film and evaporated copper. In *Plasma Surface Modification of Polymers: Relevance to Adhesion* (Strobel M, Lyons CS and Mittal KL (eds)). VSP, Utrecht, the Netherlands, pp. 275–290.
37. Rios PF, Dodiuk H, Kenig S, McCarthy S and Dotan A (2007) The effect of polymer surface on the wetting and adhesion of liquid systems. *Journal of Adhesion Science and Technology* **21(3–4)**: 227–241.
38. Christenson HK (1993) Adhesion and surface energy of mica in air and water. *Journal of Physical Chemistry* **97(46)**: 12034–12041.
39. Miao X, Gao A, Hiroto S *et al.* (2009) Adsorption characteristic of self-assembled corrole dimers on HOPG. *Surface and Interface Analysis* **41(3)**: 225–230.
40. Wang R, Sakai N, Fujishima A, Watanabe T and Hashimoto K (1999) Studies of surface wettability conversion on TiO_2 single-crystal surfaces. *Journal of Physical Chemistry B* **103(12)**: 2188–2194.
41. Yan A, Xiao X, Külaots I, Sheldon BW and Hurt RH (2006) Controlling water contact angle on carbon surfaces from 5° to 167°. *Carbon* **44(14)**: 3116–3120.
42. Liang J, Huang Y, Zhang L *et al.* (2009) Molecular-level dispersion of graphene into poly(vinyl alcohol) and effective reinforcement of their nanocomposites. *Advanced Functional Materials* **19(14)**: 2297–2302.
43. Xu Y, Hong W, Bai H, Li C and Shi G (2009) Strong and ductile poly(vinyl alcohol)/graphene oxide composite films with a layered structure. *Carbon* **47(15)**: 3538–3543.